Experimental study of time-dependent properties of a low-pH concrete for deposition tunnels

EXPERIMENTAL STUDY OF TIME-DEPENDENT PROPERTIES OF A LOW-PH CONCRETE FOR DEPOSITION TUNNELS

Alexandre Mathern[1,2], Mathias Flansbjer[3,4], Ingemar Löfgren[3,5] and Jonas Magnusson[6]

[1]PhD Student and [3]Adjunct Professor, Chalmers University of Technology, Gothenburg, Sweden
[2]Structural Engineer and [6]Lead Technical Specialist, NCC Infrastructure, Gothenburg, Sweden
[4]Researcher, RISE Research Institutes of Sweden, Borås, Sweden
[5]R&D Manager, Thomas Concrete Group (C.lab), Gothenburg, Sweden

Abstract

The Swedish Nuclear Fuel and Waste Management Company developed a method for the final disposal of canisters for spent nuclear fuel in tunnels at depths of about 500 meters. The concept for closure of the deposition tunnels is based on a bentonite seal supported by a spherical concrete dome structure. In order to fulfil the requirements specific to the repository concept, a special mix of low-pH self-compacting concrete was developed. A series of large-scale castings and laboratory tests were conducted to gain experience on this low-pH concrete mix, in conjunction with the full-scale demonstration test of an unreinforced concrete dome plug in the underground hard rock laboratory in Äspö, Sweden. The laboratory tests aimed at studying the creep properties under high sustained compressive stresses of the low-pH concrete mix, its shrinkage properties and the properties of the rock-concrete interface. This paper provides an overview of these tests and analyses the latest results of the recently completed creep tests, which include 6 years of measurements. These results allow to improve understanding of the structural behaviour of the concrete plug and to assess the effects of the very high pressure acting on the plug on its deformations, cracking and water tightness.

Keywords: Creep, Low-pH, Material properties, Self-compacting concrete, Shrinkage, Silica fume.

1. Introduction

The Swedish Nuclear Fuel and Waste Management Company (SKB) is developing a special method for the final disposal of spent nuclear fuel in tunnels at a depth of about 500 meters, as illustrated in Figure 1. This method called KBS-3V is based on three protective barriers: the copper of the canisters in which the fuel is encapsulated, a bentonite clay buffer around the canisters and the rock.

The outer sealing structure at the end of the deposition tunnels is designed as a concrete plug with a flat pressurised side towards the backfilled deposition tunnel and a spherical front side arching between recesses wire-sawn in the rock walls of the tunnel. The concrete plug aims at ensuring a watertight separation between the sealed deposition tunnels and the transport tunnels, until the transport tunnels are backfilled and the natural geohydrological conditions are restored. The concrete plug must be able to withstand the high pressure from the ground water and the swelling of the backfill clay from 90 days after casting, and this during a service life of 100 years.

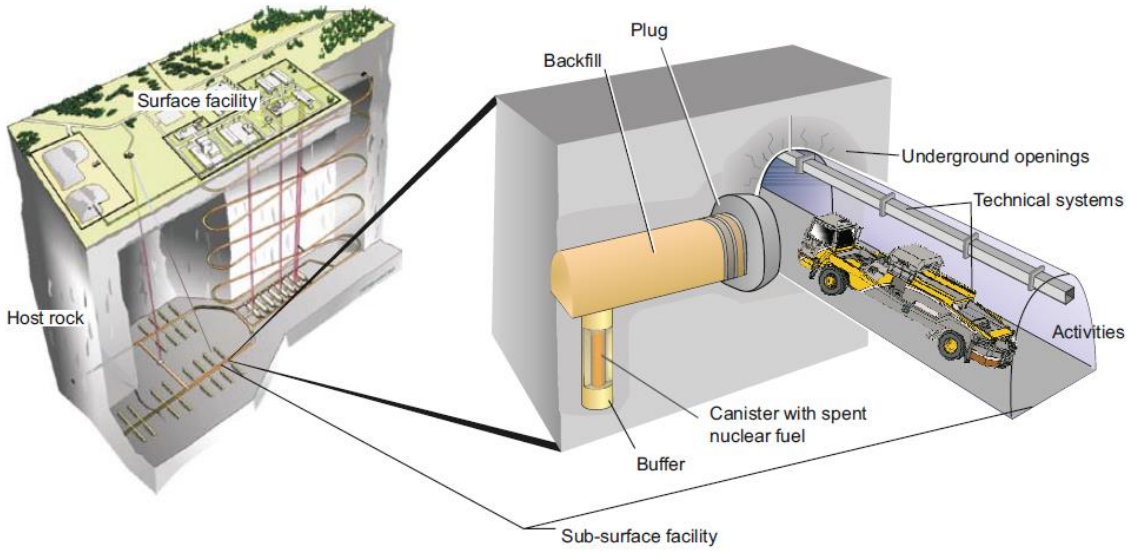

Fig. 1 Principle layout of the KBS-3V system during the operational phase (SKB, 2010).

The structure will endure a high pressure from swelling forces in the backfill clay, at present by introduction of a specially designed backfill transition zone assumed to be confined to approximately 2 MPa. However, due to the uncertainty a backfill swelling design pressure of 4 MPa has been adopted, which also shall be combined with the ground water pressure of about 5 MPa. The bentonite buffer rings around the deposited canister are sensitive to erosion. Therefore, only a very small leakage through the concrete plug is allowed, which sets strict requirements in terms of permeability.

In order to avoid possible negative effects from leachate from the concrete on the swelling properties of the bentonite, a low-pH concrete is required. Low-pH concrete is characterised by a pH below 11, while concrete normally has a pH above 12.5, and this is obtained by replacing part of the cement content by silica fume. SKB's current reference design for the concrete plug is based on the low-pH self-compacting concrete mix B200. This concrete mix was developed to fulfil the requirements specific to the repository concept.

The project KBP 1004 – System design of dome plugs for deposition tunnels, was initiated as part of the development of the KBS-3V disposal technology. A series of laboratory tests and large-scale castings were conducted within the project, from 2010 to 2018, in order to study mechanical, functional and production related aspects of the low-pH concrete mix B200.

New results obtained from creep tests are reported and analysed in this paper. The paper also provides an overview of the tests conducted on the low-pH concrete mix B200 within the KBP 1004 project.

2. Low-pH concrete mix B200

The low-pH concrete mix B200, investigated in this study, was originally developed by Vogt et al. (2009). This concrete mix was the one selected for the full-scale test of an end plug for deposition tunnels as part of the development of the KBS-3V disposal technology. The concrete mix B200 is characterized by a binder content of 200 kg per m^3 of concrete with addition of limestone powder and superplasticizer to make it self-compacting. The composition of the concrete mix B200 is given in Table 1.

Table 1. Composition of concrete mix B200.

Constituents	Amount [kg/m^3]
Anläggningscement Degerhamn CEM I 42.5 SR3 MH/LA	120
Silica fume or silica slurry[1)] (SiO_2)	80
Water	165
Limestone filler Limus 25 ($CaCO_3$)	369
Sand 0-8 mm (natural, from the Äspö area)	1037
Gravel 8-16 mm (natural or crushed)	558
Superplasticizer Glenium 51	6
TOTAL	2335

[1)] Densified silica fume was used for test series conducted in laboratory and silica slurry for the large-scale castings as it is easier to disperse and safer to handle.

Compared to conventional concrete the low-pH concrete used in this study has a very different binder system, since the binder consists of 60% Portland cement (low alkali sulfate resistant) and 40% silica fume. The pozzolanic reaction of the silica fume consumes portlandite ($Ca(OH)_2$), thus lowering the pH of the pore solution. However, the binder hydration is also accompanied by significant changes in the hydrated phases, which do not only correspond to the decrease in the portlandite content. As the pH becomes lower, monocarbonate and ettringite (AFt) become unstable (Lothenbach et al., 2011). The most significant change is probably that the C-S-H gel gets a radically different structure and composition as the ratio between calcium and silica (Ca/Si) becomes lower. With the binder composition used, as the pozzolanic reaction proceeds, the Ca/Si ratio will progressively decrease to eventually reach 1.0 or lower, compared with more than 1.6 for pure Portland cement. The low Ca/Si ratio leads to a higher degree of polymerization of the silicate chains in the C-S-H gel and also a higher content of the less strongly hydrogen-bonded water molecules in the interlayer space (García Calvo et al., 2013). The implications of this silicate polymerization and ageing of the C-S-H are that it will behave differently than a normal C-S-H for pure Portland cement and also that its properties will change with time. Experience and knowledge on the time-dependent properties of this special type of concrete are still limited.

3. Laboratory tests and large-scale castings within the KBP 1004 project

The project KBP 1004 – System design of dome plugs for deposition tunnels, was initiated as part of the development of the KBS-3V disposal technology. A series of laboratory tests and large-scale castings were conducted within the project, from 2010 to 2018, in order to study mechanical, functional and production related aspects of the low-pH concrete mix B200.

Three large-scale castings were conducted at the Äspö Hard Rock Laboratory within the framework of this project, These tests comprised a full-scale demonstration test of the plug system, with an unreinforced concrete dome plug (DOMPLU) of more than 8 m in height, conducted under realistic underground conditions in the Äspö Hard Rock Laboratory (Grahm and Malm, 2015). The main advantages of being able to perform concrete plug for deposition tunnels without reinforcement are to avoid damage caused by corrosion of the reinforcement and to prevent cracking in the plug due to restraint from the reinforcement to shrinkage of the concrete. In addition, building the concrete plug unreinforced leads to time and cost savings during installation. These large-scale castings also provided information on the properties of the fresh concrete.

Shrinkage properties and creep properties of the concrete under high stress level were studied in laboratory to gain knowledge on the structural behaviour of the concrete plug prior to and under loading. This is important in order to understand and analyse among others the long-term effects of the very high water pressure and swelling pressure on deformations, cracking and water tightness of

the unreinforced concrete plug. More details on these tests and new results from creep tests are discussed in Section 4.

The mechanical properties of the interface between the low-pH concrete B200 and the wire-sawn rock surface were also investigated at different times after casting. These properties will help to improve the understanding of the interaction between the concrete surface of the plug and the surrounding rock surface. For instance, it is important to assess the predisposition of the concrete plug will release from the rock during the hardening process of the concrete or through early cooling of the plug, especially as contact grouting is used to seal the gap between the concrete plug and the rock. These tests were conducted on cylinders, which were core-drilled from rock-concrete blocks. The blocks were manufactured in the laboratory by casting concrete against the wire sawn surfaces of rock panels from the Äspö Hard Rock Laboratory (with dimensions of approximately 800×700×150 mm). The tensile bond strength was determined by pull-off tests on cores drilled through the rock and approximately 3-4 mm into the rock. A significant difference in bond strength between vertical interface and horizontal interface was observed. The lower bond strength and the mode of failure at the interface suggest that the bond is weaker when the concrete is cast against a vertical rock surface. The shear strength of the interface and the residual shear strength of the broken interface were determined by shear load tests on cylinders core-drilled from a rock-concrete block at different constant normal stress levels, allowing to calculate the friction coefficient of the broken interface.

Some of the mechanical properties of the hardened concrete material were studied both in conjunction with the large-scale castings and in conjunction with laboratory studies of creep and interaction between concrete and rock. Hardened concrete properties were primarily tested in order to categorize and describe the concrete. However, some properties (e.g. direct tensile strength, modulus of elasticity and fracture energy) were especially studied in order to contribute to improve numerical modelling of the structural behaviour of the concrete plug.

An overview of the tests conducted on the low-pH concrete B200 within the KBP 1004 project is given in Table 2. More detailed information on the methods used for these tests and the results obtained can be found in (Magnusson and Mathern, 2015).

Table 2. Overview of the test series within the KBP 1004 project.

Test series	Conditions	Aim and material properties studied
1. Creep	Laboratory	Creep properties under high sustained stresses, corresponding to approximately 40 %, 50 % and 75 % of the 90-day compressive strength during 6 years. Mechanical properties of the concrete material in compression: *i.e.: strength development over time, effect of different storage conditions, stress-strain relation in compression and modulus of elasticity.*
2. Shrinkage	Laboratory	Shrinkage of concrete specimens under different curing conditions : at 50 % relative humidity, sealed; and in water during 3 years.
3. Interaction rock-concrete	Laboratory	Mechanical properties of the interface between the concrete and the rock: *i.e.: tensile bond strength and softening behaviour of the interface, shear strength and residual shear strength of the broken interface at different normal stress levels.* Mechanical properties of the concrete material: i.e.: *compressive strength, splitting/direct tensile strength and fracture energy.*
4. Specimen	Field	Compressive strength of concrete cubes cast at concrete plant and on site.
5. Back-wall	Field	Compressive strength of concrete cubes cast at concrete plant and on site.
6. Dome plug and concrete monolith	Field	Mechanical properties of the concrete material: - cubes cast at concrete plant and on site after 7 days, 28 days and 90 days *i.e.: compressive strength and tensile splitting strength.* - cores drilled (horizontally or vertically) at different ages from 28 days to one year *i.e.: compressive strength, splitting tensile strength and modulus of elasticity.*

4. Creep and shrinkage of the low-pH concrete B200

The high pressure endured by the concrete plug during its service life results in high long-term stresses in the concrete. The creep properties of the low-pH concrete B200 in compression were determined by tests on sealed concrete cylinders subjected to high sustained compressive longitudinal loads in mechanical rigs, as illustrated in Figure 2, according to (ASTM, 2010) and (ISO, 2009).

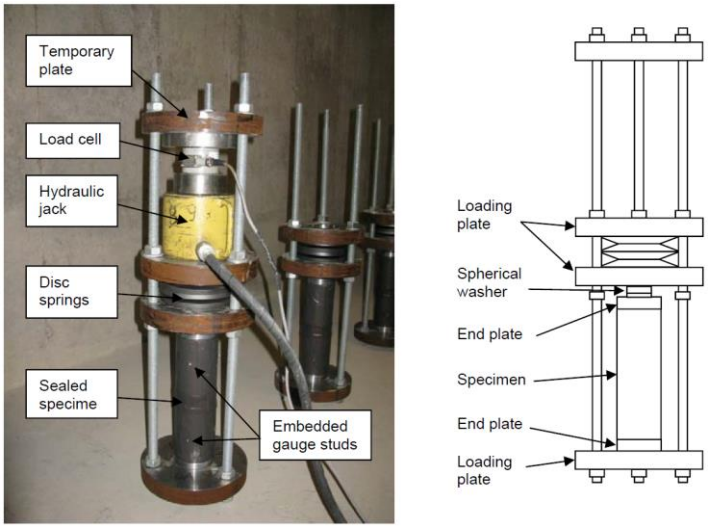

Fig. 2 Loading of a sealed creep test specimen in a mechanical rig (left) and schematic presentation of the rig (right).

The specimens were loaded at three different stress levels, approximately 40%, 50% and 75% of the compressive strength at the age of loading of approximately three months. The tests lasted 6 years, until March 2018. They were performed in two test runs; two stress levels in the first test run (TR 1a and TR 1b) and one stress level in the second test run (TR 2). Five creep specimens were loaded for each stress level and for each test run five control specimens were remained unloaded. Table 3 summarises the test programme.

The compressive strength and stress levels to be applied $\sigma_c(t_0)$ to the creep specimens were determined shortly before loading by compressive tests on concrete cubes and cylinders cast simultaneously with the casting of the creep specimens.

Tests on compressive characteristics of the concrete material were also conducted to establish strength development over time, effects of different storage conditions and stress-strain relation in compression. A more comprehensive description of the method and additional results can be found in (Flansbjer and Magnusson, 2014).

The creep of the concrete was obtained by determining the total deformation of the loaded specimens and subtracting the shrinkage of the unloaded control specimens stored in the same environmental conditions.

The total strain of the loaded creep specimens $\varepsilon_c(t)$ and the control specimens $\varepsilon_{c,control}(t)$ was calculated as the average value of the strain measurements at three lines spaced uniformly around the periphery of the specimen. The instantaneous elastic modulus $E_{ci}(t_0)$ of the creep specimens was calculated as the applied stress divided by the average strain $\varepsilon_{ci}(t_0)$ immediately after loading as:

$$E_{ci}(t_0) = \frac{\sigma_c(t_0)}{\varepsilon_{ci}(t_0)} \quad (1)$$

Table 3. Summary of creep test programme.

Test run	Dimensions	Age at time of loading t_0	Applied stress $\sigma_{cm}(t_0)$ [1]	Stress level $\sigma_{cm}(t_0) / f_{cm,cyl}$ [2]	Stress level $\sigma_{cm}(t_0) / f_{cm}$ [3]	$E_{cim}(t_0)$ [4]
	[mm]	[days]	[MPa]	[%]	[%]	[GPa]
TR 1a	Ø100×300	110	30.0	40.2	42.6	32.9
TR 1b	Ø100×300	111	38.5	51.6	54.6	32.7
TR 2	Ø90×270	91	49.4	77.3	72.0	28.9

[1] $\sigma_{cm}(t_0)$ is the average value of the applied stress $\sigma_c(t_0)$ of the specimens in the test group.
[2] $f_{cm,cyl}$ is the average compressive strength from standard cylinders Ø150×300 mm.
[3] f_{cm} is the average compressive strength from sealed cylinders of the same dimensions as the creep specimens.
[4] $E_{cim}(t_0)$ is the average instantaneous elastic modulus of the specimens in the test group.

In the first test run, the elastic modulus determined from the creep tests (see Table 3) were in the same order of magnitude as the one determined by material tests. This is expected since the applied stress levels are within the assumed elastic range. However, in the second test run the instantaneous elastic modulus from the creep test was lower than the one from the material tests. Here, the applied stress level is not in the assumed elastic range and a response corresponding to the elastic modulus from the material tests cannot be expected. A secant modulus E_c^* evaluated between 0.5 MPa and $\sigma_{cm}(t_0)$ = 49.4 MPa gives a better agreement to the instantaneous elastic modulus in the creep tests, which resulted in 31.6 GPa. In addition some creep strains may have occurred before the measurement of strains, after loading had started.

The total stress-induced strain $\varepsilon_{c\sigma}(t, t_0)$ is calculated as the difference between the average strain values of the loaded specimens and the control specimens as:

$$\varepsilon_{c\sigma}(t, t_0) = \varepsilon_c(t) - \varepsilon_{c,control}(t) \tag{2}$$

The creep strain $\varepsilon_{cc}(t, t_0)$ is calculated as the total stress-induced strain minus the strain immediately after loading as:

$$\varepsilon_{cc}(t, t_0) = \varepsilon_{c\sigma}(t, t_0) - \varepsilon_{ci}(t_0) = \varepsilon_c(t) - \varepsilon_{c,control}(t) - \varepsilon_{ci}(t_0) \tag{3}$$

The creep coefficient $\varphi(t, t_0)$ is expressed as the ratio between the creep strain and the initial strain immediately after loading:

$$\varphi(t, t_0) = \frac{\varepsilon_{cc}(t,t_0)}{\varepsilon_{ci}(t_0)} \tag{4}$$

Figure 3 presents the evolution of the mean value of the creep coefficient for each stress level. It can be seen that the higher the stress level is, the higher the creep coefficient is. In particular, the creep coefficient is increasing faster during the first days after loading for higher levels of sustained stresses. From 3 days after loading onwards, the rate of increase of the creep coefficient appears to be relatively similar for all the stress levels.

The creep coefficient appears to have stopped increasing after 4.5 years for the specimens loaded at 40% of the compressive strength. Similarly, the rate of increase of the creep coefficient seems to be very low after 5 years for the specimens loaded at 50%. The creep coefficient is still increasing significantly for the most loaded specimens (75 % stress level) after 6 years.

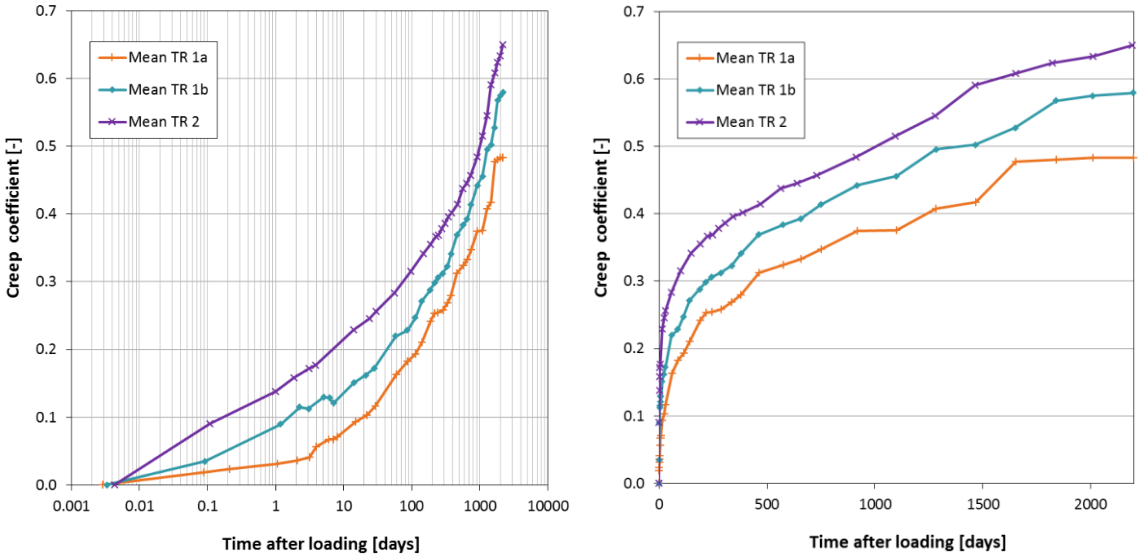

Fig. 3 Mean values of the creep coefficient versus time for TR 1a ($\sigma_{cm}(t_0)$ = 30.0 MPa), TR 1b ($\sigma_{cm}(t_0)$ = 38.5 MPa) and TR 2 ($\sigma_{cm}(t_0)$ = 49.4 MPa). The results are represented using both linear and logarithmic scales for the time to facilitate their interpretation.

Figure 4 shows a comparison between the total load-induced strains measured for each stress level and the predictions from the creep models in Model Code 2010 (fib, 2013) and Eurocode 2 (CEN, 2004). The predictions are based on the values obtained for the strength and modulus of elasticity from tests at an age of approximately 90 days and take into account the non-linearity of creep due to high stresses.

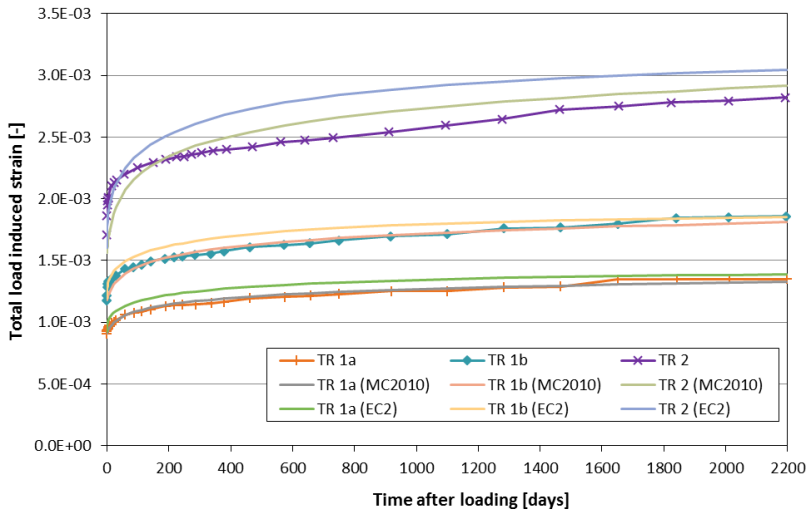

Fig. 4 Total load-induced strains versus time for TR 1a ($\sigma_{cm}(t_0)$ = 30.0 MPa), TR 1b ($\sigma_{cm}(t_0)$ = 38.5 MPa) and TR 2 ($\sigma_{cm}(t_0)$ = 49.4 MPa) and corresponding predictions from Model Code 2010 (fib, 2013) and Eurocode 2 (CEN, 2004).

The predictions from the creep models from these standards are very close to the measurements of the test series TR 1a and TR 1b, for stress levels corresponding to 40% and 50%, respectively, of the 90-day compressive strength. It indicates that it seems appropriate to use the 90-day compressive strength values for creep predictions of the low-pH concrete mix B200, according to these models. For the test series TR 2 loaded at 75% the 90-day compressive strength, the models appear to slightly overestimate the effect of high-stresses on the non-linearity of creep. It should be mentioned that

simplified formulas are given in the standards to take this effect into account, which according to Model Code 2010 (fib, 2013) are valid for stress levels up to 60% of the strength of concrete at the time of loading.

According to (fib, 2009), the ratio between the strength under sustained loading and the 28-day strength under short term loading is approximately 80% for concrete loaded at 28 days and 86% for concrete loaded at 90 days. Other studies conducted on high-performance concrete have highlighted that concrete can fail between 70% and 75% of its short term compressive strength when subjected to sustained stresses at an age of 56 days (Iravani and MacGregor, 1994). This is because the compressive strength of concrete decreases with time under high sustained compressive stresses. However, one must also keep in mind the development of strength with time due to maturation of concrete, which acts as a counteracting effect.

The load-induced strains under the maximum applied stress level reached about 0.0028 after 6 years. This strain value corresponds approximately to the strain at peak stress measured on cylinders under short-time loading in these tests series. However, higher strains can be attained in the concrete under sustained loading than under short-time loading (Iravani and MacGregor, 1994; Rüsch, 1960). Results obtained in this study within the KBP 1004 project show no indication that the stress levels applied as sustained loading will lead to failure in the concrete.

With regard to shrinkage, Figure 5 shows the results of the shrinkage tests conducted within the KBP 1004 project. These shrinkage tests were conducted on prisms of dimensions 100×100×400 mm. The tests were performed in parallel in two laboratories (CBI and C.lab) and in each laboratory 15 specimens were tested, 5 for each test series. Results from previous tests (LTU) (Vogt et al., 2009) are also shown, together with predictions from the shrinkage model in Model Code 2010 (fib, 2013) based on the 90-day concrete strength values. Shrinkage of sealed specimens seems to increase more than for normal concrete after 100 days.

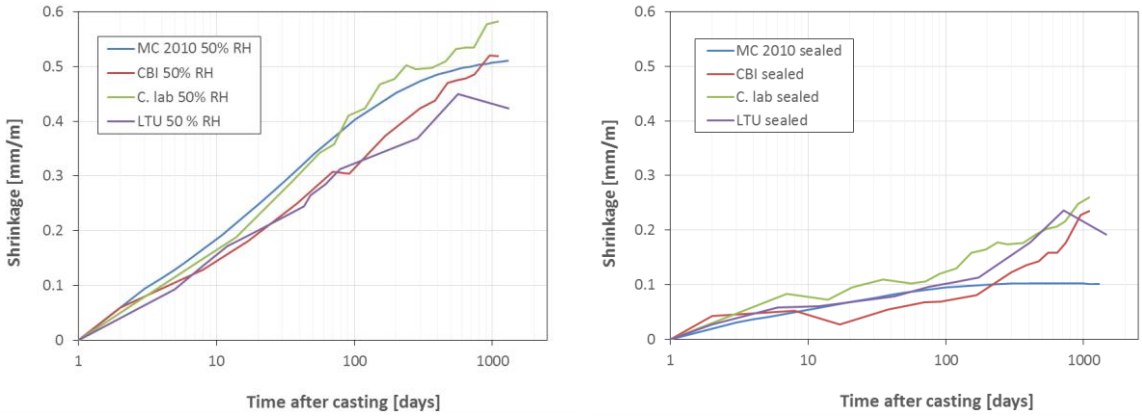

Fig. 5 Average shrinkage results from tests in different laboratories for specimens kept in 50% relative humidity (left) and sealed specimens (right) and corresponding predictions from Model Code 2010 (fib, 2013).

The shrinkage measured on the control specimens of the creep tests from 90 days after loading is very similar to the results from shrinkage tests on sealed specimens, as illustrated in Figure 6. This provides good indication of the reproducibility of the shrinkage results in different laboratories. The results also confirm that the shrinkage of the low-pH concrete B200 is still high 90 days after casting and that it continues to increasing even after more than 1000 days.

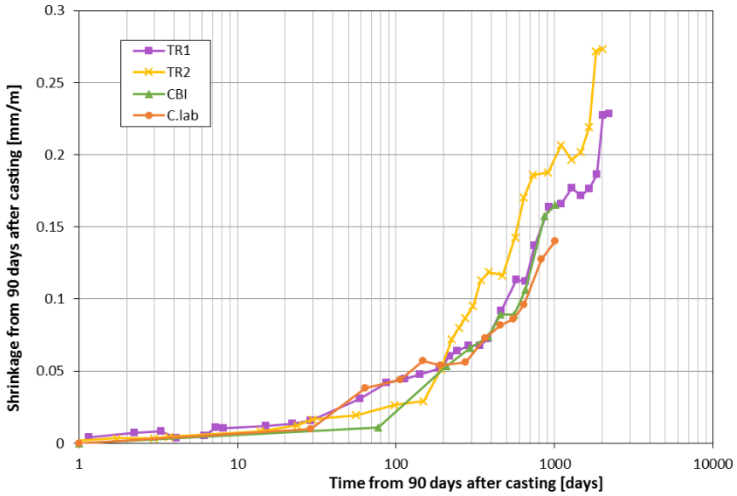

Fig. 6 Shrinkage results from 90 days after loading for sealed conditions for the control specimens (TR1 and TR2) and average results from the shrinkage tests in the KBP 1004 project (CBI and C.lab).

Chen et al. (2006) showed how the decalcification of the C-S-H, described previously in Section 2, leads to shrinkage, referred to as decalcification shrinkage. This shrinkage also occurs due to e.g. carbonation. The reason they postulated is that by removal of interlayer Ca ions in C-S-H an excess negative charge is created and this needs to be balanced by other ions (protonation) and subsequent formation of Si-OH. This may cause neighbouring Si-OH groups to condense and the mean chain length to grow (polymerization). Moreover, it was proposed that some of the siloxane bonds would form bridges between adjacent surfaces or regions, thereby contracting them and shrinking the C-S-H gel. This polymerization and shrinkage would start to occur when the Ca/Si ratio approaches 1.2. This could explain why the low pH-concrete exhibits an increased shrinkage over time, for sealed conditions, which does not occur for normal concrete. In addition, the polymerization and contraction of the C-S-H gel have been suggested to make the C-S-H stiffer and denser (Thomas and Jennings, 2006), and might explain why the creep is low and stops developing after long time for this type of concrete.

5. Conclusions

The main focus of the tests conducted in this project was to investigate further the mechanical properties of the low-pH concrete mix B200, especially from 90 days after casting onwards. The results of these tests can be divided into four categories: hardened concrete properties, shrinkage, creep, and interaction between concrete and rock.

New results from creep tests until 6 years after loading were analysed in this paper. The creep coefficient measured on the specimens loaded at 40% and 50% of the compressive strength appeared to become almost constant after 4.5 years and 5 years respectively while it was still increasing after 6 years for stress levels of 75%. The load-induced strains measured for the highest stress level reached almost 0.003 after 6 years. The results obtained show no indication that the stress levels applied as sustained loading will lead to failure in the concrete.

It was observed that the shrinkage of the low-pH concrete B200 increased over much longer time than what can be expected for normal concrete. These differences are believed to be due to decalcification shrinkage resulting from the high content of silica fume.

These results contribute to improve the understanding of the structural behaviour of the concrete plug prior to and under loading. The experimental data obtained can be used in numerical models to analyse among others the effects of the pressure on deformations, cracking and water tightness of the concrete plug.

Acknowledgment

All experimental works were carried out and financed within the research program for a future long-term nuclear fuel repository of the Swedish Nuclear Fuel and Waste Management Company (SKB).

References

ASTM, 2010. Standard test method for creep of concrete in compression. ASTM C512. ASTM International.

CEN, 2004. EN 1992-1-1:2004. Eurocode 2: Design of concrete structures - Part 1-1: General rules and rules for buildings. Brussels.

Chen, J.J., Thomas, J.J., Jennings, H.M., 2006. Decalcification shrinkage of cement paste. Cem. Concr. Res. 36, 801–809. doi:10.1016/J.CEMCONRES.2005.11.003

fib, 2013. fib Model Code for Concrete Structures 2010. International Federation for Structural Concrete.

fib, 2009. Structural concrete : textbook on behaviour, design and performance. International Federation for Structural Concrete.

Flansbjer, M., Magnusson, J., 2014. System design of Dome plug - Creep properties at high stress levels of concrete for deposition tunnel plugs. SKB P-13-37. Svensk Kärnbränslehantering AB, Stockholm, Sweden.

García Calvo, J., Sánchez Moreno, M., Alonso Alonso, M., Hidalgo López, A., García Olmo, J., 2013. Study of the Microstructure Evolution of Low-pH Cements Based on Ordinary Portland Cement (OPC) by Mid- and Near-Infrared Spectroscopy, and Their Influence on Corrosion of Steel Reinforcement. Materials (Basel). 6, 2508–2521. doi:10.3390/ma6062508

Grahm, P., Malm, R., 2015. System design and full-scale testing of the Dome Plug for KBS-3V deposition tunnels. SKB TR-14-23. Svensk Kärnbränslehantering AB, Stockholm, Sweden.

Iravani, S., MacGregor, J.G., 1994. High performance concrete under high sustained compressive stresses. Structural Engineering Report No. 200.

ISO, 2009. Testing of concrete - Part 9: Determination of creep of concrete cylinders in compression. ISO 1920-9:2009. International Organization for Standardization, Geneva, Switzerland.

Lothenbach, B., Scrivener, K., Hooton, R.D., 2011. Supplementary cementitious materials. Cem. Concr. Res. 41, 1244–1256. doi:10.1016/J.CEMCONRES.2010.12.001

Magnusson, J., Mathern, A., 2015. System design of Dome plug. SKB P-14-26. Svensk Kärnbränslehantering AB, Stockholm, Sweden.

Rüsch, H., 1960. Researches toward a general flexural theory for structural concrete. J. Am. Concr. Inst. 57, 1–28. doi:10.14359/8009

SKB, 2010. Design and production of the KBS-3 repository. SKB TR-10-12. Svensk Kärnbränslehantering AB, Stockholm, Sweden.

Thomas, J.J., Jennings, H.M., 2006. A colloidal interpretation of chemical aging of the C-S-H gel and its effects on the properties of cement paste. Cem. Concr. Res. 36, 30–38. doi:10.1016/J.CEMCONRES.2004.10.022

Vogt, C., Lagerblad, B., Wallin, K., Baldy, F., Jonasson, J., 2009. Low pH cement for deposition tunnel plugs. SKB R-09-07. Svensk Kärnbränslehantering AB, Stockholm, Sweden.